TU Delft

Delft University of Technology

Mechanical Division of Cell-Sized Liposomes

Deshpande, Siddharth; Spoelstra, Willem Kasper; Van Doorn, Marleen; Kerssemakers, Jacob; Dekker, Cees

DOI
10.1021/acsnano.7b08411

Publication date
2018

Document Version
Final published version

Published in
ACS Nano

Citation (APA)
Deshpande, S., Spoelstra, W. K., Van Doorn, M., Kerssemakers, J., & Dekker, C. (2018). Mechanical Division of Cell-Sized Liposomes. *ACS Nano*, *12*(3), 2560-2568. https://doi.org/10.1021/acsnano.7b08411

Important note
To cite this publication, please use the final published version (if applicable).
Please check the document version above.

Copyright
Other than for strictly personal use, it is not permitted to download, forward or distribute the text or part of it, without the consent of the author(s) and/or copyright holder(s), unless the work is under an open content license such as Creative Commons.

Takedown policy
Please contact us and provide details if you believe this document breaches copyrights.
We will remove access to the work immediately and investigate your claim.

This work is downloaded from Delft University of Technology.
For technical reasons the number of authors shown on this cover page is limited to a maximum of 10.

This is an open access article published under a Creative Commons Non-Commercial No Derivative Works (CC-BY-NC-ND) Attribution License, which permits copying and redistribution of the article, and creation of adaptations, all for non-commercial purposes.

ACS NANO

Cite This: ACS Nano 2018, 12, 2560−2568

www.acsnano.org

ARTICLE

Mechanical Division of Cell-Sized Liposomes

Siddharth Deshpande, Willem Kasper Spoelstra, Marleen van Doorn, Jacob Kerssemakers, and Cees Dekker*

Department of Bionanoscience, Kavli Institute of Nanoscience Delft, Delft University of Technology, Van der Maasweg 9, 2629 HZ Delft, The Netherlands

Supporting Information

ABSTRACT: **Liposomes, self-assembled vesicles with a lipid-bilayer boundary similar to cell membranes, are extensively used in both fundamental and applied sciences. Manipulation of their physical properties, such as growth and division, may significantly expand their use as model systems in cellular and synthetic biology. Several approaches have been explored to controllably divide liposomes, such as shape transformation through temperature cycling, incorporation of additional lipids, and the encapsulation of protein division machinery. However, so far, these methods lacked control, exhibited low efficiency, and yielded asymmetric division in terms of volume or lipid composition. Here, we present a microfluidics-based strategy to realize mechanical division of cell-sized (~6 μm) liposomes. We use octanol-assisted liposome assembly (OLA) to produce liposomes on chip, which are subsequently flowed against the sharp edge of a wedge-shaped splitter. Upon encountering such a Y-shaped bifurcation, the liposomes are deformed and, remarkably, are able to divide into two stable daughter liposomes in just a few milliseconds. The probability of successful division is found to critically depend on the surface area-to-volume ratio of the mother liposome, which can be tuned through osmotic pressure, and to strongly correlate to the mother liposome size for given microchannel dimensions. The division process is highly symmetric (~3% size variation between the daughter liposomes) and is accompanied by a low leakage. This mechanical division of liposomes may constitute a valuable step to establish a growth-division cycle of synthetic cells.**

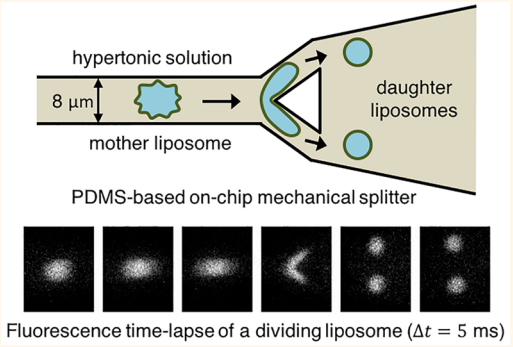

KEYWORDS: *synthetic cell division, liposomes, microfluidics, membrane biophysics, synthetic biology, octanol-assisted liposome assembly*

Cell division is one of the fundamental characteristics of living cells, responsible for the propagation of all life. Although there is wide variety of biological division mechanisms,[1−3] a universal feature of division is the production of one or more daughter cells from a mother cell, accompanied by the transfer of the genetic material to the daughter cell(s). While cell biology studies have contributed greatly to identify the complex protein machinery and signaling cascades that orchestrate this crucial biological process, *in vitro* reconstitution experiments are increasingly used to clarify cause−effect relationships therein. Multiple efforts have been initiated toward building bottom-up reconstituted systems that can induce vesicle fission.[4] Such an endeavor may significantly impact multiple scientific fields: (i) Cell biology, as such research will expand our current understanding of the cell-division machinery of prokaryotic and eukaryotic organisms. (ii) Origin of life, as protocells on the primitive earth were not yet equipped with an evolved biological machinery, yet divided, likely using some simple physical mechanism.[5] Exploring minimal ways of division will help to evaluate plausible modes of life under prebiotic conditions on the early earth. (iii) Synthetic biology, where novel forms of biotechnology are likely to emerge from the pursuit of the ultimate challenge in bottom-up synthetic biology, *viz.*, the *de novo* construction of a cell-like entity that will autonomously undergo a continuous cycle of growth, division, and evolution. Establishing efficient ways of synthetic division will be a key step in realizing these goals.

Liposomes are artificial vesicles whose membrane is composed of a phospholipid bilayer, insulating their inner aqueous lumen from the external aqueous environment. They are used in a range of applications and have proven to be an excellent model system for bottom-up synthetic biology[6] because they exhibit the universal feature of a lipid bilayer as the cell boundary and allow the encapsulation of a variety of biomolecules in the lumen or within the bilayer itself. Shape manipulation of liposomes to induce their fission has received considerable interest over the years and has been explored using a broad variety of physical, chemical, and biological strategies.[4] First evidence that it was possible to induce fission

Received: November 27, 2017
Accepted: February 18, 2018
Published: February 18, 2018

© 2018 American Chemical Society

DOI: 10.1021/acsnano.7b08411
ACS Nano 2018, 12, 2560−2568

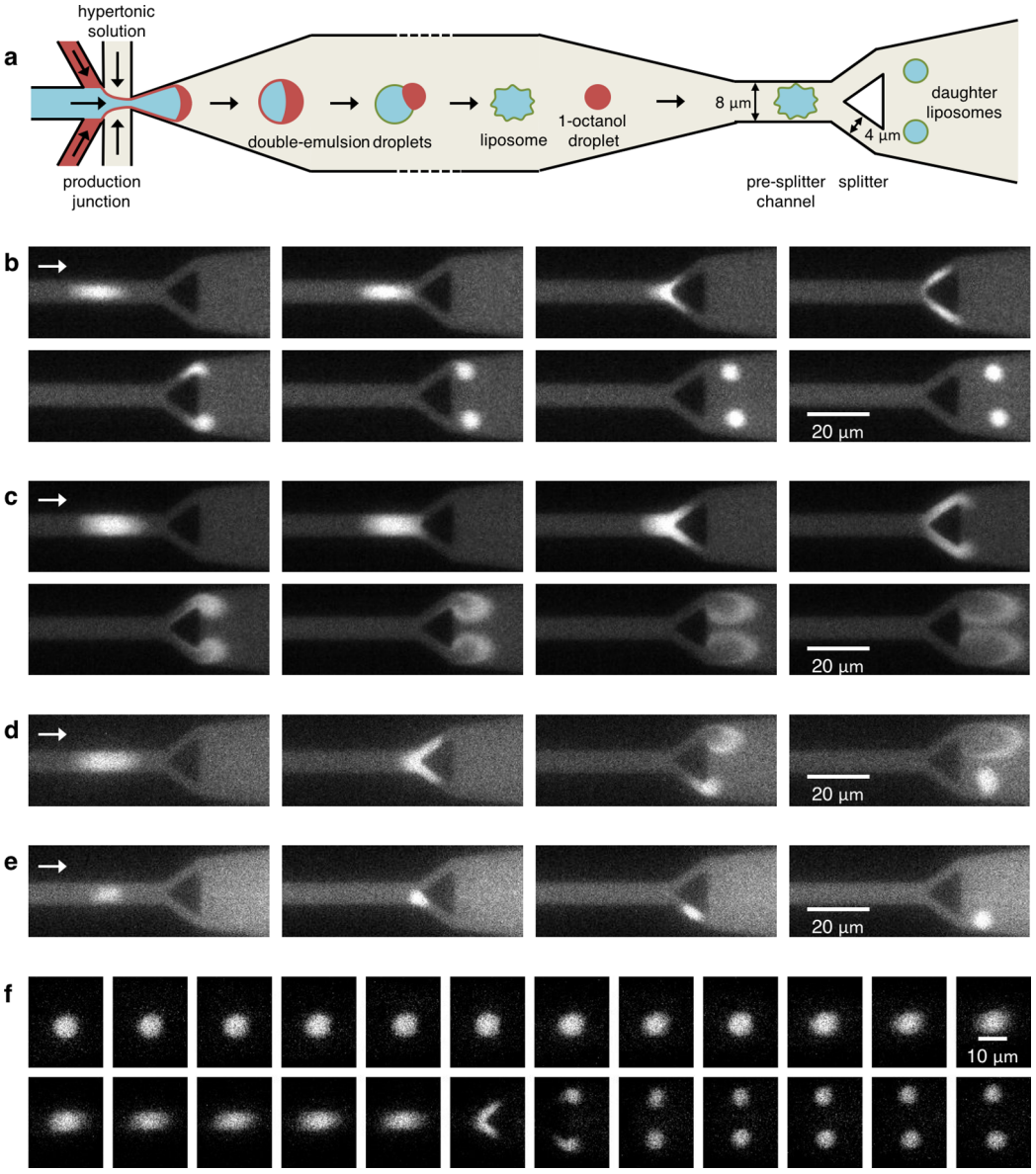

Figure 1. Mechanical division of liposomes. (a) Top-view schematic (not to scale) showing the experimental workflow leading to the mechanical division of liposomes. Double-emulsion droplets are formed at the production junction, which within minutes, mature into liposomes. By maintaining a hypertonic environment, the liposomes lose a specific volume, which sets up an intended high surface area-to-volume ratio. These "floppy" liposomes then pass through a narrow presplitter channel at a high velocity before they encounter the Y-shaped splitter, whereupon they can divide into two daughter liposomes. (b–e) Fluorescence time-lapse images (of the encapsulated dye, either Alexa Fluor 350 or Dextran-Alexa Fluor 647) showing different fates of liposomes upon encountering the splitter. (b) Division: A liposome gets deformed at the splitter and divides into two daughter liposomes. Note the similar size of the daughter liposomes indicating highly symmetric division. Also, there is no obvious increase in the background intensity after the splitting, indicating leakage-free division. (c) Bursting: Mother liposome dissociates due to the membrane rupture, spilling the inner contents into the environment. (d) Semi-division: Rarely, only one of the daughter cells survives the division process, while the other burst opens and dissociates. (e) Snaking: if small enough, the liposome passes through one of the Y-branches of the splitter, without either dividing or bursting. (f) Moving-frame region-of-interest showing an entire division event including the entry of the liposome into the narrow presplitter channel. The images underwent appropriate background subtraction, and further analyses were performed with similarly processed images. The lipid composition of liposomes is DOPC and Rh-PE (molar ratio of 99.9:0.1). Time difference Δt between successive frames is $\Delta t_{division}$ = 1.2 ms (panel b), $\Delta t_{bursting}$ = 1.2 ms (panel c), $\Delta t_{semi\text{-}division}$ = 3 ms (panel d), $\Delta t_{snaking}$ = 4 ms (panel e), $\Delta t_{moving\text{-}frame}$ = 2 ms (panel f). Horizontal arrows indicate the flow direction. Mother liposomes appear deformed in the presplitter channel due to motion blurring.

of giant unilamellar vesicles (GUVs, diameter >1 μm) came from increasing their surface area-to-volume ratio by elevating the temperature above the phase transition temperature of the lipids.[7] Along similar lines, heating–cooling cycles across the phase transition temperature were shown to induce inward/outward budding and subsequent fission.[8,9] Another route involved forming coexisting lipid domains of liquid-ordered and liquid-disordered phases, and minimizing the line tension at the boundary to bring about vesicle fission.[10,11] Division can also be induced by incorporating lipids or fatty acids into the liposomal membrane,[12−15] or by providing surplus membrane to liposomes.[16] A more biological approach can be undertaken

DOI: 10.1021/acsnano.7b08411
ACS Nano 2018, 12, 2560−2568

by encapsulating the minimal bacterial divisome machinery inside a liposome. Upon encapsulating key bacterial proteins such as FtsZ and its membrane anchor FtsA, constriction was reported in small unilamellar vesicles (SUVs, diameter <100 nm),[17] while division was observed at a very low efficiency (<1%) in GUVs.[18] Apart from these strategies, mechanical shearing, by extrusion of vesicles through a membrane of defined pore size, is extensively used for the preparation of monodispersed SUVs.[19]

All these strategies suffer from two key problems: (i) Lack of control: the division process in these methods is generally not very predictable and has a low efficiency. (ii) Asymmetry: The division is asymmetric in terms of volume, as the volume of the mother liposome gets divided unequally over two or more daughter liposomes. It can also be asymmetric in terms of the lipid composition, leading to an unequal lipid composition of the daughter cells. Although asymmetric division mechanisms have evolved in both eukaryotes and prokaryotes,[2,3] achieving symmetric division is advantageous from the point of view of equal distribution of the inner contents and thus the prospect of a simple continuous growth-division synthetic cell cycle. From our overview of results reported so far, we conclude that a method for controlled, efficient, and symmetric division of cell-sized liposomes is lacking.

In this paper, we report a different strategy to achieve liposome division where we use microfluidics to apply mechanical force to cut liposomes in half. We use our recently developed microfluidic liposome-production method, octanol-assisted liposome assembly (OLA), to generate cell-sized, monodisperse, unilamellar liposomes inside microfluidic channels.[20] We then collide these OLA-generated liposomes against the edge of a wedge-shaped splitter at high velocity (a few mm/s) (Figure 1). This leads to pronounced shape deformations of liposomes that surprisingly allow them to divide into two equal daughter liposomes under specific conditions. We show that such division is possible only when the liposome is tuned to have an excess surface area to compensate for the change in surface area-to-volume ratio associated with the formation of two smaller daughters compared to the original large mother liposome. Also, the size of the liposomes, with respect to the microchannel dimensions, is found to strongly influence their fate: liposomes which are too small simply pass through one of the splitter branches of the Y-junction, while too big liposomes undergo an overly severe deformation and burst open. Only medium-sized liposomes are well set up to face the deformation at the splitter and successfully divide into two daughter liposomes. The division process is found to be highly symmetric (only 3% variation in the diameter of the daughter liposomes) and accompanied by low leakage (~10%). Our microfluidic splitter technique thus provides a simple way to achieve symmetric, efficient, quick, and protein-free division of cell-sized liposomes. Such a liposome manipulation technique provides an excellent tool in bottom-up synthetic biology, and it also can be utilized to achieve rapid production of smaller liposomes through amplification.

RESULTS

We produced unilamellar liposomes (4−10 μm in diameter) using OLA.[20] In a process akin to bubble-blowing, OLA involves the formation of double-emulsion droplets (water droplets encapsulated within a shell of lipids dissolved in 1-octanol, suspended in an aqueous environment) at the production junction (Figure 1a), whereupon, within minutes, these double-emulsion droplets spontaneously separate into liposomes and 1-octanol droplets. This mixture of liposomes and 1-octanol droplets steadily flows in the post-junction microfluidic channel with a velocity set by the pressure exerted at the production junction. Simultaneously, we decreased the volume of the liposomes by creating an osmotic pressure difference across the membrane in order to make the division possible; see details mentioned later in the text. At a sufficient distance from the production junction, where most of the double-emulsion droplets have given rise to liposomes, we bifurcated the microfluidic channel into two smaller channels (each 4 μm wide, at an angle θ = 70° with respect to each other), forming a Y-shaped junction, termed "splitter" from now on (Figure 1a). Just before the splitter, the width of the channel was narrowed to 8 μm, while the height of the channels was about 7.5 μm for the entire device. For visualization, we used high-speed fluorescence microscopy (up to 1000 frames per second), and doped the liposomal bilayer membrane with a small fraction of fluorescent lipids. At the same time, we also encapsulated a fluorescent dye inside the liposomes (see Methods).

As a liposome entered the narrow pre-splitter channel, it encountered the splitter with a collision velocity of 5−10 mm/s. Due to its deformability, the liposome did not stall at the splitter, but changed its shape, as it flowed past the junction. We categorized the events that followed the encounter between the liposomes and the splitter into four different types, *viz.*, division, bursting, semi-successful division, and snaking, which are described as follows.

Division. In these events, the liposomes got stretched symmetrically across the two branches of the splitter and subsequently divided into two intact daughter liposomes (Figure 1b; Supplementary Movie S1 and Supplementary Movie S2). The division time, defined as the time between the first contact of the liposome with the splitter and its separation into two stable, unconnected daughter liposomes, was very brief, amounting to only a few milliseconds. The formed daughter liposomes were not deformed but spherical in appearance, and flowed downstream of the splitter. The sharp front edge of the splitter thus simply acted as a mechanical cutter to bring about liposome division. Figure 1b shows an example of such a division event where the fluorescence emitted from the lumen of the liposome was recorded. Additionally, Figure 1f shows a processed moving-frame image sequence where an initially spherical liposome enters the narrow pre-splitter channel and gets cut at the splitter into two daughter liposomes. Further analyses were performed on such processed image sequences (see Methods for details).

Bursting. Here, the initial deformation of the liposome over the two branches of the splitter looked similar to the division event. By contrast, however, the deformed mother liposome ruptured before daughter liposomes were able to form (Figure 1c, Supplementary Movie S3). As the membrane was disrupted, presumably due to a critically increased surface tension, the inner contents of the liposome leaked out and diffused into the environment.

Semi-division. In rare cases, only one daughter liposome survived the splitting process, while the other one burst, resulting in a semi-successful division process (Figure 1d, Supplementary Movie S4).

Snaking. In these events, the mother liposome was not observed to split into progeny but instead slipped as one entity

DOI: 10.1021/acsnano.7b08411
ACS Nano 2018, 12, 2560−2568

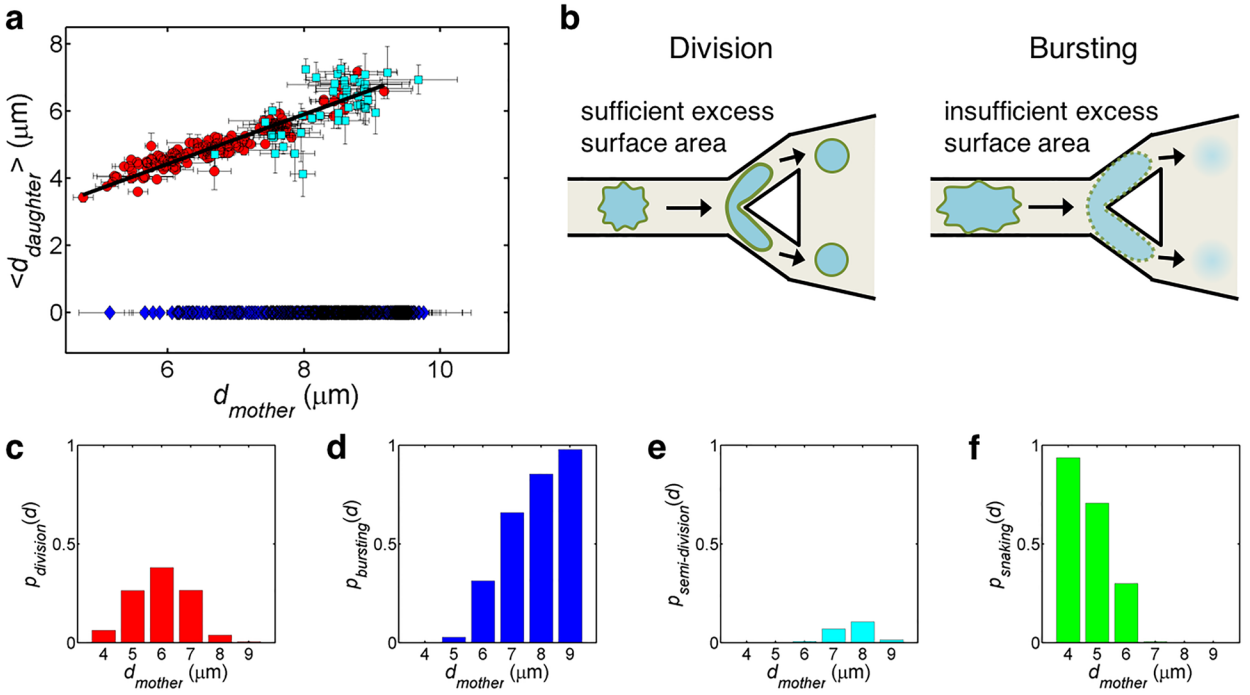

Figure 2. Liposome fate upon encountering the splitter is determined by its size. (a) Mean diameter of daughter liposomes against that of corresponding mother liposomes. Red circles represent division events, while cyan squares represent semi-divisions. The line shows a linear fit with a slope m = 0.74 ± 0.01 (mean ± s.d., R^2 = 0.89). For bursts (dark blue diamonds), data points are displayed at the horizontal axis, since no daughter liposomes were formed. Horizontal and vertical error bars indicate corresponding standard deviations. $N_{division}$ = 151, N_{burst} = 602, $N_{semi\text{-}division}$ = 46. (b) Top-view schematics explaining how liposome size affects the splitting probability. A small enough liposome is moderately stretched at the splitter but still has enough excess surface area required for division. For a bigger liposome, the decrease in excess surface area is more drastic, thus increasing the probability of bursting. (c–f) The probability of different events, *viz.*, division (c), bursting (d), semi-division (e), and snaking (f) as a function of liposome diameter, obtained from the experimental data ($N_{division}$ = 151, N_{burst} = 602, $N_{semi\text{-}division}$ = 46, N_{snake} = 159). The value of each bar denotes the fraction of the specific event occurring for that particular liposome diameter. Channel dimensions were kept constant, and the impact velocity varied within a similar range for all the events.

through one of the two splitter branches (Figure 1e, Supplementary Movie S5). This usually happened for small liposomes with a diameter that was similar to the size of the Y-branches, as one would intuitively expect.

Finally, we note that 1-octanol droplets and not-yet-separated double-emulsion droplets (*i.e.*, liposomes still connected to an octanol droplet) also successfully split at the splitter (Supplementary Figure S1, Supplementary Movie S6). Droplet division, however, is a fundamentally different process, and has been reported before.[21]

Dividing a spherical mother liposome into two spherical daughter liposomes is challenged by the fundamental problem that both a constant surface area (set by the amount of lipids in the mother liposome) and conserved volume (in the absence of any leakage) must be maintained. Yet, the surface area-to-volume ratio is different for two small spheres compared to one large one, and hence it intrinsically will be different before and after the splitting of a spherical liposome. As a consequence, division is not possible without either a loss of volume or a gain in the surface area. Some gain in surface area can be realized by stretching the membrane, but only a limited expansion (~5%) can be realized.[22,23] Potentially, one can increase the surface area by inducing vesicle fusion,[24] or by incorporation of external lipid molecules into the existing lipid bilayer of the mother liposome.[13,14] These are, however, very difficult routes to implement near the splitter on a millisecond time scale. Hence, we sought a simpler solution: reducing the volume of the mother liposome. The volume of a liposome can in fact be precisely tuned by inducing an appropriate osmotic pressure difference across its semipermeable membrane. Thus, by decreasing the volume of the mother liposome by extracting an appropriate amount of water from it, it should be possible to create enough excess surface area to fit the division requirement.

Concretely, for the symmetric division of a mother liposome with volume V_0, area A_0, and radius R_0 into two smaller liposomes each having radius r, the constraint of area conservation, $A_0 = 4\pi R_0^2 = 2 \times 4\pi r^2$ dictates that $r = (R_0/\sqrt{2})$, *i.e.*, the daughters have a radius that is $(1/\sqrt{2}) \approx 0.71$ times that of the mother. Hence, the target volume V_0 of the mother liposome must be reduced beforehand by a factor α, which is deduced from the volume conservation in the division, *i.e.*, $\alpha(4/3)\pi R_0^3 = 2 \times (4/3)\pi r^3 \rightarrow \alpha = (1/\sqrt{2}) \approx 0.71$. This simple analysis shows that we needed to decrease the volume of mother liposomes beforehand from its perfect spherical volume by 29%, using osmotic control. We experimentally tuned α by using a hypertonic environment, having a surplus of sucrose compared to the liposomal lumen, right from the start of the liposome production ($[\text{sucrose}_{lumen}]/[\text{sucrose}_{environment}] \approx 0.7 \rightarrow \alpha \approx 0.7$) (Figure 1). Unintended rupture of some double-emulsion droplets and liposomes reduced the external sucrose concentration slightly, yielding an actual value of α that we estimated to be around 0.76 (see Supplementary Note S1). Nonetheless, as previously discussed, liposomes can tolerate a limited area expansion, providing enough margin for the division to take place. Deliberately decreasing the value of α to

DOI: 10.1021/acsnano.7b08411
ACS Nano 2018, 12, 2560–2568

0.65, in order to compensate for the experimental rise, did not lead to a more efficient liposome production and thus was not pursued further. On the basis of a previously developed permeability model,[25] the time needed for the liposome to reach osmotic equilibrium with its environment was estimated to be less than 20 s (Supplementary Note S2, Supplementary Figure S2). Since it took more than 2 min for the liposome to reach the splitting geometry in the experiments, it can be safely assumed that the liposomes reached osmotic equilibrium before hitting the splitter, allowing the volume to be decreased appropriately. As expected, when we instead bombarded the liposomes against the splitter under isotonic conditions (without any osmotic pressure difference, *i.e.*, no sucrose gradient across the membrane), liposome division was never observed. Instead, bursting or snaking events were obtained over the whole size range of mother liposomes (Supplementary Figure S3).

We quantitatively analyzed the four distinct types of events, to check the frequency of occurrence, the symmetry, and the leakage involved in the splitting process. Figure 2a shows a plot of the mean diameter of daughter liposomes against that of the corresponding mother liposomes (see Methods for diameter estimation). For division events, a strong linear correlation was obtained between the two (R^2 = 0.89), with the diameter of the daughter liposomes being about 0.74 times that of their corresponding mother liposomes (slope m = 0.74 ± 0.01; mean ± standard deviation, s.d.). This value is close to what one would expect for a symmetric division. In order to investigate the correlation between liposome size and its fate at the splitter, we plotted the probability of different events as a function of the mother liposome diameter (Figure 2c–f). The frequency histograms of the corresponding size distributions for the different events is given in Supplementary Figure S4. As can be seen in Figure 2c, the probability of a successful division ($p_{division}$) follows a bell-shaped curve, with a peak value at about 6 μm. For lower (<5 μm) as well as higher diameters (>7 μm), $p_{division}$ rapidly decreases to zero. Snaking events are prominent for the smallest liposomes, d_{mother} = 4–6 μm (Figure 2f). On the other hand, the probability of bursting ($p_{bursting}$) increases sharply with size, becoming the majority event for $d_{mother} \geq 7$ μm (Figure 2d). Semi-divisions, which are very rare events, occur exclusively for $d_{mother} \geq 7$ μm (Figure 2e).

Such a distinct probability distribution for different events clearly demonstrates the role of liposome size relative to the dimensions of the microchannels in which it is confined, in determining the liposome fate as it collides with the splitter. If the value of liposome diameter is similar to the width of the Y-branches, it can simply squeeze through one of the branches without getting obstructed at the splitter. On the other hand, a bigger liposome gets symmetrically stretched out across both channels of the splitter (Figure 2b) and can potentially split into two daughter liposomes. We expect the division to occur only if the liposome has enough excess surface area to compensate for the surface area increase due to the stretching at the splitter. Indeed, when a middle-sized liposome (*e.g.*, 6 μm in diameter) gets stretched across the splitter, its surface area increases marginally (~7%, see Methods for details), and the liposome is still able to divide since the stretching is much less that the excess surface area (~27%) induced by the osmotically regulated volume reduction. In case of a larger liposome (*e.g.*, 8 μm in diameter), however, the increase in the surface area is more drastic (~28%) as the liposomes is stretched across the splitter. This makes the division less likely, as the membrane ruptures and the liposome bursts (Figure 2b). Thus, the upper limit on the size of the mother liposome for a successful division is a result of a compromise between allowing for enough deformation of the mother liposome and not putting it under too much mechanical stress. We also checked whether different fates of liposomes correlated with the collision velocity, but no such correlation was found within the narrow range of collision velocities with which the liposomes hit the splitter (between 5 to 10 mm/s; Supplementary Figure S5). Lastly, the splitter angle did not seem to be of much significance for the mechanical division of liposomes, as a substantial change in its value (θ = 30°) also led to liposome division and comparable probability distributions for different events (Supplementary Figure S6).

Next, we quantified the symmetry involved in the division process, *i.e.*, how similar the daughter liposomes are in terms of their size and the encapsulated material. Figure 3a shows the

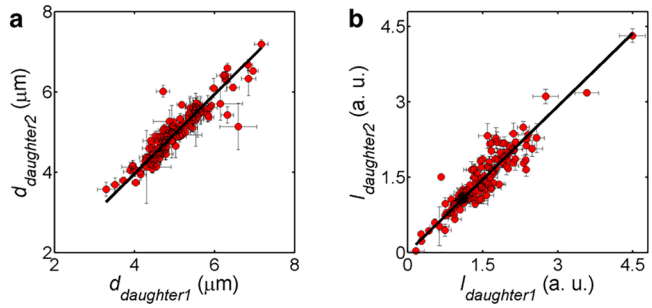

Figure 3. Mechanical division of liposomes is highly symmetric. (a) Plot showing the correlation between the diameters of the daughter liposomes, resulting from the same mother liposome. The linear fit, shown by the line, has a slope of 0.99 ± 0.01 (mean ± s.d., R^2 = 0.88), emphasizing the highly symmetric nature of the division process. (b) Plot showing the correlation obtained between the total intensity of the two daughter liposomes obtained from the same mother liposome. The solid line, which is a linear fit to the data set, has a slope of m = 0.97 ± 0.01 (mean ± s.d., R^2 = 0.86), indicating an equal distribution of the encapsulated material during the division process. Horizontal and vertical error bars indicate corresponding standard deviations. In total, 152 (panel a) and 151 (panel b) pairs of daughter liposomes were analyzed.

diameters of the daughter liposomes plotted against each other, for each daughter pair from the same mother liposome. A slope of 0.99 ± 0.01 (mean ± s.d.; R^2 = 0.88) indicates that the physical splitting of the liposomes is highly symmetric, on average leading to two daughter liposomes of the same size. In order to quantify the size variation between daughter liposomes, we define a (conservatively chosen) symmetry parameter as $s = (d_{small}/d_{big})$, where d_{small} is the diameter of the smaller daughter liposome and d_{big} is that of the bigger daughter liposome. From our data, we calculated s = 0.97 ± 0.03 (mean ± s.d.), reflecting, on average, a mere 3% coefficient of variation in the size of the two daughter liposomes. Figure 3b shows the correlation between the total fluorescence counts from the two daughter liposomes. Again, a slope of 0.97 ± 0.01 (mean ± s.d.; R^2 = 0.86) indicates that the daughter liposomes have a nearly identical concentration of dye molecules encapsulated within their lumen.

An important aspect of the splitting process is the leakage involved, *i.e.*, to what extent the encapsulated molecules in the mother vesicle are transferred to the two daughter liposomes. For both natural and synthetic cells, it is important that division

DOI: 10.1021/acsnano.7b08411
ACS Nano 2018, 12, 2560–2568

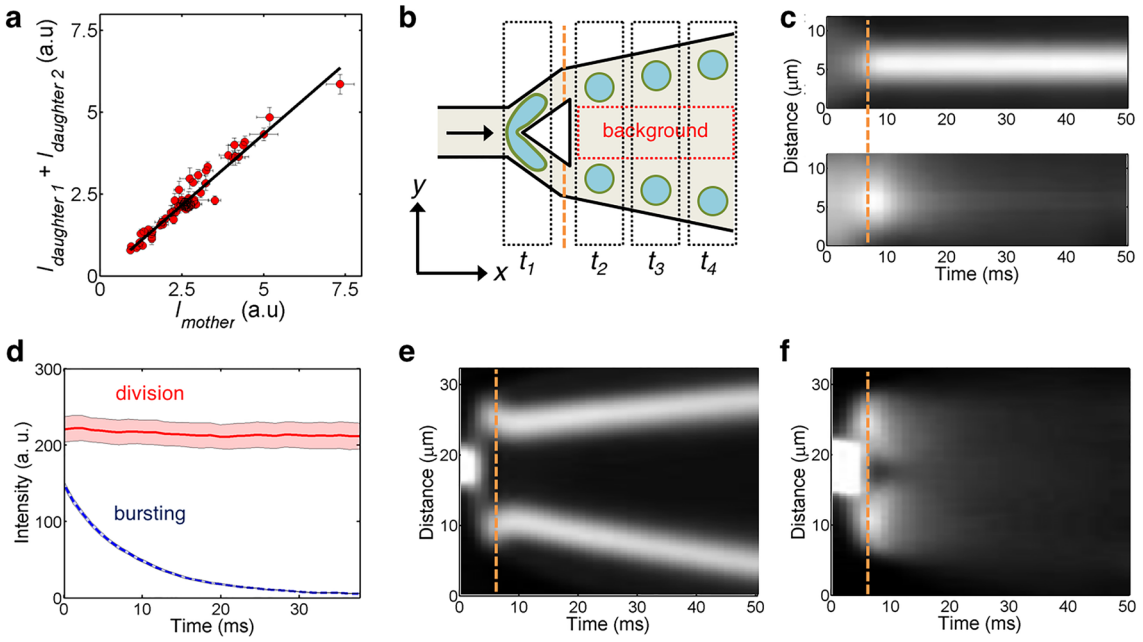

Figure 4. Liposome division is associated with a low leakage. (a) Plot of the total intensity of daughter liposomes against that of the corresponding mother liposomes (N = 78). The intensities are strongly correlated, with the solid line showing a linear fit with a slope of m = 0.87 ± 0.01 (mean ± s.d., R^2 = 0.94), suggesting a leakage of 13% during the division process. Horizontal and vertical error bars indicate corresponding standard deviations. (b) Top-view schematic showing a dividing liposome at different time points. Summing up the fluorescence intensity along the x- (or y) axis for each region-of-interest generates a moving-frame x−t (or y−t) kymograph. (c) Average x−t kymographs for division (upper, N = 131) and bursting (lower, N = 199) events. The x−t kymograph of dividing liposomes gives a straight bright trace, while that of bursting liposomes results in a rapidly fading trace. (d) Average intensity profile stays constant in case of division (red solid line), while decays rapidly in case of bursting (blue dashed line). The plots are obtained from the corresponding average moving-frame x−t kymographs. The shaded regions indicate the standard deviations. (e−f) Average moving-frame y−t kymograph of division events (e) which clearly shows a constant dark background confirming a very low amount of leakage involved in the division process (N = 131). In comparison, a similar kymograph for bursting events (f) shows a considerable rise in the background as the encapsulated dye diffuses away into the environment (N = 199). The vertical dashed lines in b, c, e and f indicate the splitter position. Contrast has been enhanced for better visualization.

occurs in as leakage-free manner as possible, to avoid the loss of vital cellular components. A straightforward way to calculate the leakage is to compare the fluorescence intensity of the mother to that of the two daughter liposomes combined, where the difference indicates the leakage involved. Figure 4a shows the total fluorescence intensity counts of both daughter liposomes combined, against the total intensity of the corresponding mother liposomes. We obtained a robust linear correlation (R^2 = 0.94), with a slope m = 0.87 ± 0.01 (mean ± s.d.), suggesting a leakage of 13%. Note that this value remained unchanged after using a correction factor, *i.e.*, coincidentally the correction factor equaled 1 (*viz.*, effectively no correction). The correction factor accounted for two opposing effects, namely a background correction that amended for the dependence of obtained fluorescence counts on channel geometry, and an optical correction that amended for the dependence of obtained fluorescence counts on object size (see Methods). Summing up, we estimated a low leakage during the division process, on the order of 10%.

To further corroborate the low leakage involved in the division process, we quantified the increase in the background intensity in the external environment, just after the division took place. First, we built moving-frame movies of individual liposomes by cutting a region-of-interest around the liposome for each time point (t_1, t_2, ...), as indicated in Figure 4b. Using these movies, we built kymographs by summing up the fluorescence intensity of each movie frame, along either the x- or the y-axis. By summing up the intensity along the x-axis, *i.e.*, parallel to the pre-splitter channel, we obtained average x−t kymographs for division as well as bursting events (Figure 4c). Plotting the intensity profile across the x−t kymograph for division events showed a nearly constant fluorescence intensity for the liposomes (Figure 4d, solid red line), confirming low leakage. By contrast, the bursting events show a rapid decay (Figure 4d, dashed blue line). By summing up the intensity along the y-axis, *i.e.*, perpendicular to the pre-splitter channel, we obtained average y−t kymographs for division (Figure 4e) and bursting events (Figure 4f). A y−t kymograph of a dividing liposome generated a horizontal line that bifurcated after the splitter, while the y−t kymograph of a bursting liposome produced a straight line until the splitter position, after which it fades due to the diffusion of the leaked fluorescent molecules. As can be clearly observed, there is no appreciable change in the background intensity for the division kymographs, while in case of bursting kymographs, the dissociation of liposome is evident from the diffusion of the fluorescent dye into the environment. In order to check whether the divided liposomes were stable over long periods of time, we obtained images of divided and snaked liposomes after a substantial time interval (>1 h) after the division (see Supplementary Figure S7). These images clearly show that encapsulated fluorescent molecules did not leak out from the liposomes and no long-lasting pores were formed during or after the division process. High-resolution images that visualize the liposome membrane clearly showed the intact nature of the membrane. Overall, we conclude that

DOI: 10.1021/acsnano.7b08411
ACS Nano 2018, 12, 2560−2568

the mechanically induced division of liposomes is accompanied by a low leakage.

CONCLUSIONS

In this paper, we have described an efficient and simple method to divide cell-sized (~6 μm) liposomes in a highly symmetric and a low-leakage manner. By flowing the liposomes onto a Y-shaped junction at high flow velocity, we could efficiently divide them into two daughter liposomes, with a low leakage (~10% of the volume) and excellent symmetry (~3% variation in the diameter). This division was facilitated by inducing an osmotic pressure difference across the membrane of the mother liposome, in order to reduce its volume by about 30% before the division, so as to account for the different surface area-to-volume ratio of the daughter vesicles as compared to the mother vesicle. In absence of such a controlled volume reduction, we did not observe divisions but only bursting and snaking of liposomes.

How does the division occur exactly? There are two distinct possibilities for the mechanism that underlies the mechanical liposome division that is observed. Splitting may occur through a hemifission mechanism: As the liposome gets strongly deformed at the Y-junction, it is pushed sideways to both splitter channels, and the two bilayers at the front and back end of the deformed liposome are forced to approach and perhaps even touch each other at the tip of the splitter. This direct contact may lead to a hemifission process, changing the topology of the connecting bilayers. This would constitute a splitting process with a high chance for a completely leakage-free fission. Notably, protein-free hemifusion (which is the opposite of hemifission) has been experimentally verified and shown to be dependent on sufficiently close interbilayer contact.[26] Alternatively, however, division may occur through a break-seal mechanism. In this scenario, the liposome flows against the Y-junction, and gets strongly deformed. As it continues to get stretched, the lipid bilayer breaks, most likely on the posterior sides where the local stress is most pronounced, and two daughter liposomes are formed that each have a transient open pore. These pores subsequently reseal and give rise to intact daughter liposomes. It has been experimentally observed that increasing the membrane tension of a liposome can indeed result in a transient pore that reseals itself if sufficient inner content leaks out to release the tension.[27] Unfortunately, the imaging resolution does not allow to rigorously distinguish by what mechanism the liposomes undergo physical division. The small but finite leakage observed in our experiments suggests that the break-seal division mode underlies the splitting process.

Mechanical division of liposomes can be advantageous for several applications. Similar to the system developed for single- and double-emulsion amplification through division,[21] mechanical liposome division could, in principle, be used to exponentially amplify the number of liposomes. Since the volume of daughter liposomes halves at every division, the methodology presented here suggests a way to cover a broader size range, and potentially form submicrometer-sized liposomes. This may open up the possibility of using OLA-based liposomes as drug delivery systems, since optimal drug carriers are in the submicrometer range.[28] It could also be effective to place the splitter right after the production junction, in order to first divide the double-emulsion droplets (which is an efficient and robust process as can be seen from Supplementary Movie S6) and then let the liposomes mature upon subsequent separation of 1-octanol droplets. As with any technique, the mechanical division approach also has its limitations. For example, this approach might prove difficult to apply to multicomponent vesicles. Also, the liposomes may contain trace amount of 1-octanol present in the membrane.

One of the foreseeable aims in synthetic biology is to establish a primitive life cycle of vesicles that grow and divide in a recurring manner. In order to obtain such a cycle, the symmetric nature of the division (both in terms of volume and lipid composition) is advantageous. Furthermore, the division should be as leakage-free as possible, since loss of low-copy-number information-carrying molecules like ribonucleic acids may render daughter cells unviable. The presented scheme for mechanical division of liposomes makes highly symmetric liposomes that are capable of potentially undergoing repeated division cycles, when combined with a growth module. The presented strategy of using a mechanical force to induce shape manipulations and achieve protein-free division may also have implications in the origin-of-life research. In absence of complex biological machinery, protocells on early earth likely relied on physical shear forces, such as fluid currents and migration through narrow solid confinements (*e.g.*, in clay), in order to produce offspring. As has been shown before for the case of fatty acid vesicles,[29−31] we show here that a purely mechanical division of lipid-based vesicles is also indeed possible, providing support for such a mode of protocell division.

Future research may expand in many directions. For example, by creating asymmetric splitting junctions, one can investigate how the symmetry of division is affected by the symmetry of the splitter. Simulations, along with ultrahigh-spatiotemporal-resolution images of the division process, could shed further light on the details of the division process, possibly distinguishing between the proposed hemifission and the break-seal mechanisms. As lipid composition is known to play a crucial role in membrane fusion and fission,[26] it will be interesting to see the effect of different membrane compositions on the splitting efficiency. So far, it was not possible to significantly modulate the flow velocity, since the splitter is directly connected to the production junction. Using a recently developed density-based liposome separation technique which decouples the production and further downstream experimentation,[32] it will be possible to vary the collision velocity of the liposomes, and investigate its effect on the splitting efficiency. Finally, combining the physical division with a growth module to achieve a growth-division cycle will be a significant step in the context of synthetic biology.

METHODS

Liposome Production Using OLA. Please refer to our online protocol for further details and troubleshooting of OLA.[33]

LO (Lipid-Containing 1-Octanol) Phase Preparation. Lipids, dissolved in chloroform, were purchased from Avanti Polar Lipids. Chloroform was evaporated by passing a gentle stream of argon or nitrogen, and the lipids were further dried by desiccating for at least 2 h. A stock concentration (100 mg/mL) was prepared by dissolving the lipids in ethanol and stored at −20 °C under inert gas atmosphere. 1,2-dioleoyl-*sn*-glycero-3-phosphocholine (DOPC) was used as the lipid source. A fluorescent lipid, 1,2-dioleoyl-*sn*-glycero-3-phosphoethanolamine-*N*-(lissamine rhodamine B sulfonyl) (Rh-PE) was added for visualization (DOPC:Rh-PE = 99.9:0.1, molar ratio). During experiments, the stock solution was dissolved in 1-octanol (Sigma-Aldrich Co.) to a final concentration of 2 mg/mL.

DOI: 10.1021/acsnano.7b08411
ACS Nano 2018, 12, 2560−2568

Soft Lithography. Patterns were fabricated in silicon, using e-beam lithography and dry etching procedure, as described elsewhere.[20] Additionally, after etching, the wafer was cleaned in the inductive coupled plasma (ICP) reactive-ion etcher (Adixen AMS 100 I-speeder) at a pressure of 0.04 mbar, ICP power set at 2500 W with a biased power of 60 W, a source-target distance of 200 mm, temperature set at 10 °C, and using O_2 gas at 200 sccm for 3−5 min. The height of the etched-structures was measured using a stylus profiler, DektakXT (Bruker Corporation) and was 7.5 μm. Finally, the wafer was cleaned with acetone, rinsed in deionized water and spin-dried. The wafer surface was then rendered antiadhesive by exposing it to (tridecafluoro-1,1,2,2-tetrahydrooctyl) trichlorosilane (abcr GmbH & Co.) in partial vacuum for at least 12 h.

Microfluidic devices were made by pouring polydimethylsiloxane (PDMS), mixed with a curing agent (Sylgard 184, Dow Corning GmbH) at a mass ratio 10:1, on the wafer and baking at 80 °C for at least 4 h. The PDMS block was then peeled off from the wafer and holes were punched into it using a biopsy punch (World Precision Instruments, inner diameter 0.77 mm). The PDMS block was then cleaned with isopropanol and dried under a stream of nitrogen. Glass slides were also coated with a thin PDMS layer as described previously.[20] The PDMS block and the PDMS-coated glass slide were then exposed to oxygen plasma for ∼10 s (3−4 SCFH O_2, 200 W) using a Plasma-Preen system (Plasmatic Systems, Inc.). Immediately after the plasma treatment, the glass slide was bonded to the PDMS block. The device was further baked at 80 °C for ∼20 min. Microfluidic flow control system (positive pressure: 0−1000 mbar, Fluigent GmbH) along with the MAESFLO software (version 3.2.1) were used to flow the solutions into the microfluidic device using appropriate metal connectors (BD microlance needles, outer diameter 0.6 mm, cut into ∼1 cm pieces) and tubing (Tygon Microbore Tubing, inner diameter 0.51 mm).

Surface Treatment and Experimentation. Channels downstream of the liposome-producing junction were rendered hydrophilic by adsorbing poly(vinyl alcohol) (PVA) polymers (Sigma-Aldrich) to the PDMS surface, as described elsewhere.[20]

Image Acquisition and Processing. An Olympus IX81 inverted microscope equipped with epifluorescence illumination, appropriate filter sets, a 20× (UPlanSApo, numerical aperture 0.75) objective (Olympus), and a 60× (PlanApoN, numerical aperture 1.45, oil) objective (Olympus) were used to perform the experiments. The images were recorded using a Neo sCMOS camera or a Zyla 4.2 PLUS CMOS camera (Andor Technology), and a micromanager software (version 1.4.14).[34]

In the recorded movies, liposomes appeared as bright objects while 1-octanol droplets/pockets appeared as dark objects. The background was faintly fluorescent, due to unintended rupturing events upstream of the splitter and/or due to the low concentration of fluorescent molecules present in the environment (Supplementary Movie S2). The background fluorescence helped to rule out the false-positive division events, where a 1-octanol pocket was still attached to the liposome as it encountered the splitter. Image processing was performed with MATLAB, using self-written scripts (see Supplementary Figure S8 for a typical example). Briefly, high-speed movies capturing the fluorescence from the encapsulated dye were used to track bright objects in the successive movie frames, using a particle detection-and-tracing routine. The resulting position-time traces were classified depending on the nature of the events (division, burst, semi-division, snake), while the difference between traces yielded local velocities. Screening was done to remove erroneous traces (*e.g.*, two different mother liposomes detected within a single position-time trace). This was done by plotting the ratio of the major and the minor axis of the daughter liposomes (A_{maj}/A_{min}), against the intensity ratio of daughter and mother liposomes ($I_{daughter}/I_{mother}$). This led to event-specific clusters; data points lying beyond two standard deviations ($\pm 2\sigma$) from the mean value of that particular event (μ) were removed. Only the first frames, before the liposome entered the narrow pre-splitter channel, were used for the measurement of total fluorescence counts, area, major axis, and minor axis. In this way, any effects of motion-blurring and physical deformation at the junction were avoided. The contribution of the background dye to the fluorescence of the liposome was minimized by subtracting the movie median from each movie image. Further data processing was performed on regions-of-interest (ROIs) around the object cut from the movie frames. For each ROI, a second background subtraction was performed using the lowest value detected inside the microfluidic channel.

Each data point is plotted as an average, its value obtained from several consecutive ROIs. Fluorescent intensity of liposomes was obtained by summing up all the counts above 10% of the peak value, to avoid inclusion of random background fluctuations. For measurements of area, major axis, and minor axis, a binary image of the fluorescent signal was used, with the threshold set at the half-maximum value. Diameter, either for free liposomes or when the liposome was squeezed into a disc-like shape inside the microfluidic channel, was calculated from the area as described elsewhere.[20] To estimate the increase in the surface area of the mother liposome as it got stretched at the splitter, the liposome was approximated as an ellipsoid, with one principal semi-axis, a = 2 μm (Y-branch width/2) and the second semi-axis, b = 3.75 μm (channel height/2). The third semi-axis c was calculated as $(3V/4\pi ab)$, where V is the liposome volume that was calculated by considering the liposome as a non-stretched sphere of the mentioned diameter. The surface area was then approximated as $4\pi((ab^{1.6} + ac^{1.6} + bc^{1.6})/3)^{(1/1.6)}$.

Estimation of the Correction Factor for Comparing Mother and Daughter Liposome Intensities. We found that, even after a straightforward background subtraction, the resulting fluorescence counts were still sensitive to the location where the object was analyzed, whether it was in the pre-splitter part or the wider post-splitter part of the channel. To compensate for this intensity difference due to the channel geometry, a background correction factor (c_1) was introduced using snaking events as a reference. During snaking, liposomes simply flowed across the splitter through one of the Y-branches, and thus were safely assumed to be leakage-free events. Plotting the intensities of snaking liposomes before and after the splitter gave the value of c_1 = 0.90 (Supplementary Figure S7).

Furthermore, in order to account for the influence of the object size on the obtained fluorescence counts, an additional optical correction factor (c_2) was introduced. To quantify this dependence for a leakage-free system, we analyzed the division of 4−8 μm 1-octanol droplets (Supplementary Figure S10). These droplets, being single-emulsions, undergo a completely leakage-free division at the splitter. A clear linear relationship between the total fluorescence counts of the two daughter droplets against the corresponding mother droplets was obtained, yielding c_2 = 1.11 (Supplementary Figure S10b). The total correction factor was thus calculated as $c = c_1c_2$ = 1.00.

Solution Compositions. All the solutions were purchased from Sigma-Aldrich, except Dextran-Alexa Fluor 647 (Molecular Weight 10 000) which was purchased from Thermo Fisher Scientific. OLA requires the presence of Poloxamer 188 (P188), a nonionic triblock copolymer surfactant, which weakly adsorbs on the membrane surface.[35] Since P188 does not insert itself into the membrane, it is highly unlikely that its presence is crucial for a successful liposome division.

Inner aqueous phase consisted of 15% v/v glycerol, 5% w/v P188, fluorescent molecules (either 98 μM Alexa Fluor 350 or 16 μM Dextran-Alexa Fluor 647), and sucrose (58 mM or 70 mM), dissolved in pure water. Lipid-carrying organic phase was 0.2% w/v lipids (99.9 mol % DOPC + 0.1 mol % Rh-PE) in 1-octanol. Outer aqueous phase was made up of 15% v/v glycerol, 5% w/v P188, optional fluorescent molecules (4 μM Dextran-Alexa Fluor 647), and sucrose (82 mM or 100 mM), dissolved in pure water. Sucrose concentrations in the two aqueous phases were chosen so that α = 0.7. In case of negative control, no sucrose or 100 mM sucrose was present in both the inner and the outer aqueous phase.

ASSOCIATED CONTENT

Supporting Information

The Supporting Information is available free of charge on the ACS Publications website at DOI: 10.1021/acsnano.7b08411.

DOI: 10.1021/acsnano.7b08411
ACS Nano 2018, 12, 2560−2568

Notes S1−S2; Figures S1−S10 (PDF)
Movie S1 (AVI)
Movie S2 (AVI)
Movie S3 (AVI)
Movie S4 (AVI)
Movie S5 (AVI)
Movie S6 (AVI)

AUTHOR INFORMATION

Corresponding Author

*E-mail: c.dekker@tudelft.nl.

ORCID

Siddharth Deshpande: 0000-0002-7137-8962
Cees Dekker: 0000-0001-6273-071X

Author Contributions

S.D., K.S., and C.D. conceived the experiments. K.S., M.D., and S.D. performed the experiments. J.K., S.D., K.S., and M.D. analyzed the data. S.D. and C.D. wrote the paper.

Notes

The authors declare no competing financial interest.

ACKNOWLEDGMENTS

We would like to thank F. Fanalista, A. Birnie, and T. Idema for help and fruitful discussions. This work was supported by the NWO TOP-PUNT Grant (No. 718014001), The Netherlands Organisation for Scientific Research (NWO/OCW), and European Research Council Advanced Grant SynDiv (No. 669598).

REFERENCES

(1) Angert, E. R. Alternatives to Binary Fission in Bacteria. *Nat. Rev. Microbiol.* **2005**, *3*, 214−224.
(2) Kysela, D. T.; Brown, P. J.; Casey Huang, K.; Brun, Y. V. Biological Consequences and Advantages of Asymmetric Bacterial Growth. *Annu. Rev. Microbiol.* **2013**, *67*, 417−435.
(3) Macara, I. G.; Mili, S. Polarity and Differential Inheritance-Universal Attributes of Life? *Cell* **2008**, *135*, 801−812.
(4) Caspi, Y.; Dekker, C. Divided We Stand: Splitting Synthetic Cells for Their Proliferation. *Syst. Synth. Biol.* **2014**, *8*, 249−269.
(5) Szostak, J. W.; Bartel, D. P.; Luisi, L. Synthesizing Life. *Nature* **2001**, *409*, 387−390.
(6) Fenz, S. F.; Sengupta, K. Giant Vesicles as Cell Models. *Integr. Biol.* **2012**, *4*, 982.
(7) Döbereiner, H. G.; Käs, J.; Noppl, D.; Sprenger, I.; Sackmann, E. Budding and Fission of Vesicles. *Biophys. J.* **1993**, *65*, 1396−1403.
(8) Sakuma, Y.; Imai, M. Model System of Self-Reproducing Vesicles. *Phys. Rev. Lett.* **2011**, *107*, 1−5.
(9) Leirer, C.; Wunderlich, B.; Myles, V. M.; Schneider, M. F. Phase Transition Induced Fission in Lipid Vesicles. *Biophys. Chem.* **2009**, *143*, 106−109.
(10) Baumgart, T.; Hess, S. T.; Webb, W. W. Imaging Coexisting Fluid Domains in Biomembrane Models Coupling Curvature and Line Tension. *Nature* **2003**, *425*, 821−824.
(11) Andes-Koback, M.; Keating, C. D. Complete Budding and Asymmetric Division of Primitive Model Cells to Produce Daughter Vesicles with Different Interior and Membrane Compositions. *J. Am. Chem. Soc.* **2011**, *133*, 9545−9555.
(12) Rasi, S.; Mavelli, F.; Luisi, P. L. Cooperative Micelle Binding and Matrix Effect in Oleate Vesicle Formation. *J. Phys. Chem. B* **2003**, *107*, 14068−14076.
(13) Inaoka, Y.; Yamazaki, M. Vesicle Fission of Giant Unilamellar Vesicles of Liquid-Ordered-Phase Membranes Induced by Amphiphiles with a Single Long Hydrocarbon Chain. *Langmuir* **2007**, *23*, 720−728.
(14) Tanaka, T.; Sano, R.; Yamashita, Y.; Yamazaki, M. Shape Changes and Vesicle Fission of Giant Unilamellar Vesicles of Liquid-Ordered Phase Membrane Induced by Lysophosphatidylcholine. *Langmuir* **2004**, *20*, 9526−9534.
(15) Kurihara, K.; Okura, Y.; Matsuo, M.; Toyota, T.; Suzuki, K.; Sugawara, T. A Recursive Vesicle-Based Model Protocell with a Primitive Model Cell Cycle. *Nat. Commun.* **2015**, *6*, 8352.
(16) Terasawa, H.; Nishimura, K.; Suzuki, H.; Matsuura, T.; Yomo, T. Coupling of the Fusion and Budding of Giant Phospholipid Vesicles Containing Macromolecules. *Proc. Natl. Acad. Sci. U. S. A.* **2012**, *109*, 5942−5947.
(17) Szwedziak, P.; Wang, Q.; Bharat, T. A. M.; Tsim, M.; Löwe, J. Architecture of the Ring Formed by the Tubulin Homologue FtsZ in Bacterial Cell Division. *eLife* **2014**, No. e04601, DOI: 10.7554/eLife.04601.
(18) Osawa, M.; Erickson, H. P. Liposome Division by a Simple Bacterial Division Machinery. *Proc. Natl. Acad. Sci. U. S. A.* **2013**, *110*, 11000−11004.
(19) Olson, F.; Hunt, C. A.; Szoka, F. C.; Vail, W. J.; Papahadjopoulos, D. Preparation of Liposomes of Defined Size Distribution by Extrusion through Polycarbonate Membranes. *Biochim. Biophys. Acta, Biomembr.* **1979**, *557*, 9−23.
(20) Deshpande, S.; Caspi, Y.; Meijering, A. E.; Dekker, C. Octanol-Assisted Liposome Assembly on Chip. *Nat. Commun.* **2016**, *7*, 10447.
(21) Abate, A. R.; Weitz, D. a. Faster Multiple Emulsification with Drop Splitting. *Lab Chip* **2011**, *11*, 1911−1915.
(22) Hallett, F. R.; Marsh, J.; Nickel, B. G.; Wood, J. M. Mechanical Properties of Vesicles. II. A Model for Osmotic Swelling and Lysis. *Biophys. J.* **1993**, *64*, 435−442.
(23) Oglęcka, K.; Rangamani, P.; Liedberg, B.; Kraut, R. S.; Parikh, A. N. Oscillatory Phase Separation in Giant Lipid Vesicles Induced by Transmembrane Osmotic Differentials. *eLife* **2014**, No. e03695, DOI: 10.7554/eLife.03695.
(24) Haluska, C. K.; Riske, K. A.; Marchi-Artzner, V.; Lehn, J.-M.; Lipowsky, R.; Dimova, R. Time Scales of Membrane Fusion Revealed by Direct Imaging of Vesicle Fusion with High Temporal Resolution. *Proc. Natl. Acad. Sci. U. S. A.* **2006**, *103*, 15841−15846.
(25) Olbrich, K.; Rawicz, W.; Needham, D.; Evans, E. Water Permeability and Mechanical Strength of Polyunsaturated Lipid Bilayers. *Biophys. J.* **2000**, *79*, 321−327.
(26) Chernomordik, L. V.; Kozlov, M. M. Mechanics of Membrane Fusion. *Nat. Struct. Mol. Biol.* **2008**, *15*, 675−683.
(27) Karatekin, E.; Sandre, O.; Guitouni, H.; Borghi, N.; Puech, P.-H.; Brochard-Wyart, F. Cascades of Transient Pores in Giant Vesicles: Line Tension and Transport. *Biophys. J.* **2003**, *84*, 1734−1749.
(28) Carugo, D.; Bottaro, E.; Owen, J.; Stride, E.; Nastruzzi, C. Liposome Production by Microfluidics: Potential and Limiting Factors. *Sci. Rep.* **2016**, *6*, 25876.
(29) Hanczyc, M. M.; Fujikawa, S. M.; Szostak, J. W. Experimental Models of Primitive Cellular Compartments: Encapsulation, Growth, and Division. *Science* **2003**, *302*, 618−622.
(30) Zhu, T. F.; Szostak, J. W. Coupled Growth and Division of Model Protocell Membranes. *J. Am. Chem. Soc.* **2009**, *131*, 5705−5713.
(31) Budin, I.; Szostak, J. W. Physical Effects Underlying the Transition from Primitive to Modern Cell Membranes. *Proc. Natl. Acad. Sci. U. S. A.* **2011**, *108*, 5249−5254.
(32) Deshpande, S.; Birnie, A.; Dekker, C. On-Chip Density-Based Purification of Liposomes. *Biomicrofluidics* **2017**, *11*, 34106.
(33) Deshpande, S.; Dekker, C. On-Chip Microfluidic Production of Cell-Sized Liposomes. *Nat. Protoc.* **2018**, in press.
(34) Edelstein, A.; Amodaj, N.; Hoover, K.; Vale, R.; Stuurman, N. Computer Control of Microscopes Using μManager. *Curr. Protoc. Mol. Biol.* **2010**, 14.20 DOI: 10.1002/0471142727.mb1420s92.
(35) Cheng, C. Y.; Wang, J. Y.; Kausik, R.; Lee, K. Y. C.; Han, S. Nature of Interactions between PEO-PPO-PEO Triblock Copolymers and Lipid Membranes: (II) Role of Hydration Dynamics Revealed by Dynamic Nuclear Polarization. *Biomacromolecules* **2012**, *13*, 2624−2633.

DOI: 10.1021/acsnano.7b08411
ACS Nano 2018, 12, 2560−2568